Hybrid MPC for gasoline engine air-fuel ratio control using optimal PWA approximation

Marek Honek, Martin Gulan, Cristina Vlad, Boris Rohaľ-Ilkiv

Hybrid MPC for gasoline engine air-fuel ratio control using optimal PWA approximation

Marek Honek * **Martin Gulan** * **Cristina Vlad** **
Boris Rohaľ-Ilkiv *

* *Institute of Automation, Measurement and Applied Informatics; Faculty of Mechanical Engineering; Slovak University of Technology in Bratislava; Námestie slobody 17; 812 31 Bratislava; Slovakia (e-mail: marek.honek@stuba.sk, martin.gulan∼, boris.rohal-ilkiv∼).*
** *Laboratory of Signals and Systems; CentraleSupélec-CNRS-Univeristé Paris Sud, Univeristé Paris-Saclay; 3 rue Joliot Curie; 911 90 Gif-sur-Yvette; France (e-mail: cristina.vlad@centralesupelec.fr).*

Abstract: This paper deals with air-fuel ratio control for a gasoline combustion engine. The proposed approach is based on tracking of fuel mass flow reference using a nonlinear model of air and fuel path dynamics in cylinder. To maintain the model accuracy while keeping its complexity on an acceptable level, we propose to employ an optimal piecewise affine approximation of the derived nonlinear model, covering the entire operating range of the real system. The resulting hybrid model is subsequently used for model predictive control synthesis, where the formulated optimization problem is solved online by mixed-integer quadratic programming. To evaluate the tradeoff between complexity and performance of the obtained controller, it is compared with the one obtained by nonlinear programming exploiting the full nonlinear model. The simulation results show that even a relatively low-complex approximation leads to a satisfactory air-fuel ratio control performance while allowing for potential practical implementation on a real engine.

Keywords: gasoline engine, air-fuel ratio control, piecewise affine model, hybrid model predictive control

1. INTRODUCTION

Over the last few decades the ever-decreasing cost/power ratio of micorcontroller units and memory chips has enabled the car manufacturers to implement more and more advanced and computationally demanding control strategies. Starting with the most basic ones—using static maps and PID feedback loops from sensors—to optimal, model-based control strategies, on all levels of hierarchical control system with the aim to increase comfort, reliability, safety, and decrease energy consumption and thus safe cost and environment. The problem of air-fuel ratio (AFR) control plays an important role in the complex problem of emission reduction for combustion engines. Quality of the air-fuel mixture is essential for the efficiency of a three-way catalytic converter, and therefore suitable control techniques are needed to fulfil the emission legislations.

The highest efficiency of a three way catalytic conversion is achieved for fuel mixture with AFR on stoichiometric level. Only for a very narrow band of AFR around stoichiometric level, three main pollutant species in exhaust gas, namely hydrocarbon (HC), carbon monoxide (CO) and nitrogen oxide (NO_x), can be almost completely converted to the innocuous components, water (H_2O) and carbon dioxide (CO_2)(Guzzella and Onder, 2010).

Conventional feedback control loops taking measurements of AFR using the lambda sensor in exhaust manifold do not provide satisfying control performance due to the presence of transport delay. To overcome this problem, AFR control strategies tend to employ open-loop observers in order to determine the amount of fuel which needs to be injected, proportionally to the air mass entering the cylinder. These observers can be implemented using either maps or models, and their action is corrected by an appropriately designed feedback loop, typically PID, in order to reject steady-state errors possibly occurring in presence of model uncertainties, parameter variations caused by engine aging, and/or changes of ambient conditions (Guzzella and Onder, 2010; Eriksson and Nielsen, 2014).

Apart from the air charge estimation problem, Shen et al. (2015) comprehensively describe the problem of fuel path dynamics compensation. The authors also propose a Lyapunov-based adaptive control method allowing to address the problem with inaccuracies in the air charge estimation and the fuel path dynamics compensation, resulting from the wide operating range of the engine, the inherent nonlinearities of the combustion process, the large modeling uncertainties, and the parameter variations. Another interesting AFR control approach was proposed e.g. in Rupp

⋆ The authors gratefully acknowledge the contribution of the Slovak Research and Development Agency (APVV) under the contracts APVV-14-0399, APVV-0015-12 and APVV SK-FR-2015-0015.

and Guzzella (2010), where authors designed an internal model controller with adaptation to aging lambda sensor. Since the air and fuel path dynamics of a gasoline combustion engine are varying with dependency on engine speed and throttle position, linear parameter-varying techniques are very often sought for the design of an AFR controller. In Zope et al. (2010), the authors propose a parameter-dependent state feedback controller using Lyapunov stability approach. A different approach, utilizing model predictive control based on a parameter-dependent weighting of local linear models was proposed in Wojnar et al. (2013).

Model predictive control (MPC) has experienced a growing success since the middle of the 1980's for complex plants with rather slow dynamics, mainly in chemical and process industry. It has become a very popular optimization-based control strategy due to its ability to guarantee optimal performance while taking constraints into account. Applicability of MPC based strategies for automotive applications has been extensively studied in del Re et al. (2009). Fast nonlinear MPC (NMPC) schemes have been adopted for several AFR control applications, as it is reported in Wang et al. (2006); Zhai et al. (2007, 2011). Recently, in Honek et al. (2015) the authors proposed a design methodology to obtain a low-complexity explicit MPC for AFR control in the vicinity of one operating regime. Validity of such controller could be potentially extended by devising a suitable switching strategy among neighboring controllers.

In order to cover the entire operating range of a gasoline combustion engine in a more systematic manner, we herein focus on design of hybrid MPC for AFR control. Instead of using the complex full nonlinear model of air and fuel path dynamics in cylinder, we propose to employ an optimal piecewise affine approximation (PWA) of the derived nonlinear model, as outlined in Kvasnica et al. (2011). The obtained PWA model is subsequently used for synthesis of an MPC controller, where the underlying optimization problem is solved online with mixed-integer quadratic programming (miQP). To assess the tradeoff between complexity and performance of the resulting AFR controller, we compare it with the one obtained with nonlinear programming (NLP) exploiting the full nonlinear model, and illustrate the control concept via simulation results.

2. NONLINEAR ENGINE MODEL

The naturally aspired gasoline engine represents a strongly nonlinear system. The air flow is controlled by position of the electronic throttle's plate, α_{ref}, and the fuel flow by fuel injector's opening time, t_{inj}. This kind of engine is usually equipped with a mass (air) flow sensor (MAF) that enables to directly measure the air mass flow through the throttle, $\dot{m}_{\text{th}}$, and/or with intake manifold pressure and temperature sensors where measurements taken from these sensors can be used for estimation of air mass flow into the cylinder, $\dot{m}_{\text{ac}}$. Information of AFR measured by the λ-sensor, located in the confluence point of exhaust manifold, is usually used for feedback AFR control loop. The above concepts are illustrated in Fig. 1.

The mean value engine model (MVEM) of a gasoline engine, presented in this section, is adopted from Hendricks and Sorenson (1990); Manzie et al. (2002); Eriksson and Nielsen (2014). In particular, it describes a naturally aspired engine with port fuel injection system. As depicted in Fig. 2, three dynamic phenomena have to be considered when modeling this kind of engine. Dynamics of the air path is given by dynamics of the electronic throttle and intake manifold filling dynamics, see Eqs. (1) and (4) (Eriksson and Nielsen, 2014). On the other hand, presence of the fuel path dynamics stems from the fact that fuel is injected on closed inlet valves of cylinders, which gives rise to the wall wetting effect, see Eqs. (8) (Manzie et al., 2002). Another dynamic effect occurs while the gas travels from the cylinder to the λ-sensor located in the confluence point of exhaust manifold. As the gases mix along the pipe, it smooths out variations in the exhaust gases.

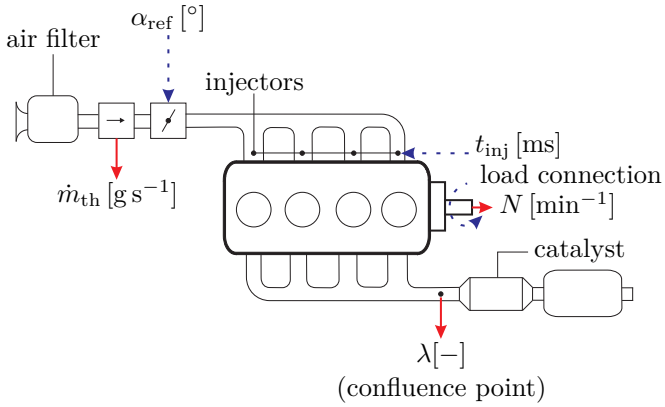

Fig. 1. Engine setup with input/output relations; dashed arrows – inputs, solid arrows – outputs

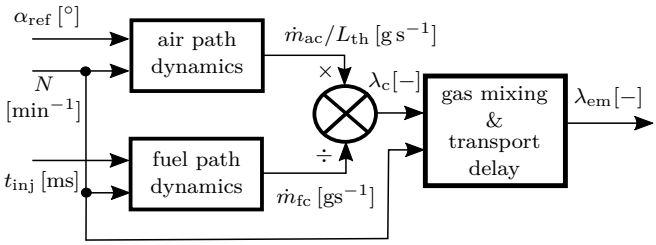

Fig. 2. Block scheme of an SI combustion engine

2.1 Air path dynamics

The first modelled subsystem of the air path, describing relation between the reference, α_{ref}, and the actual position, α, of the throttle plate is given by the first order system (1). Time constant τ_{th} amounts to 0.03 s which is given by the requirement on the settling time of the throttle plate's position control.

$$\dot{\alpha}(\alpha_{\text{ref}}, \alpha) = \frac{1}{\tau_{\text{th}}}(\alpha_{\text{ref}} - \alpha) \tag{1}$$

Under the assumptions that the area of throttle plate shaft is neglected, the throttle plate is infinitely thin, the pipe of the throttle body is circular with diameter D_{th}, throttle is fully closed at $\alpha = 0°$ and fully opened at $\alpha = 90°$, the throttle area A_{th} can be simply determined by the following equation:

$$A_{\text{th}}(\alpha) = \frac{\pi D_{\text{th}}^2}{4}(1 - \cos\alpha), \tag{2}$$

i.e. as the difference between area of a circle and an ellipse. The model of the isentropic compressible flow suitable for

modeling of air mass flow through throttle $\dot{m}_{\mathrm{th}}$ is given by following system of equations:

$$\Pi\left(\frac{p_{\mathrm{im}}}{p_{\mathrm{amb}}}\right) = \max\left(\frac{p_{\mathrm{im}}}{p_{\mathrm{amb}}}, \left(\frac{2}{\gamma_{\mathrm{air}}+1}\right)^{\frac{\gamma_{\mathrm{air}}}{(\gamma_{\mathrm{air}}-1)}}\right), \tag{3a}$$

$$\Psi_0\left(\Pi\right) = \sqrt{\frac{2\gamma_{\mathrm{air}}}{\gamma_{\mathrm{air}}-1}\left(\Pi^{\frac{2}{\gamma_{\mathrm{air}}}} - \Pi^{\frac{\gamma_{\mathrm{air}}+1}{\gamma_{\mathrm{air}}}}\right)}, \tag{3b}$$

$$\Psi_{\mathrm{lin}}(\Pi) = \begin{cases} \Psi_0\left(\Pi\right) & \text{if } \Pi \leq \Pi_{\mathrm{lin}}, \\ \Psi_0\left(\Pi_{\mathrm{lin}}\right)\dfrac{1-\Pi}{1-\Pi_{\mathrm{lin}}} & \text{otherwise,} \end{cases} \tag{3c}$$

$$\dot{m}_{\mathrm{th}}(p_{\mathrm{im}}, A_{\mathrm{th}}) = A_{\mathrm{th}}\frac{p_{\mathrm{amb}}}{\sqrt{RT_{\mathrm{amb}}}}\Psi_{\mathrm{lin}}(\Pi\left(\frac{p_{\mathrm{im}}}{p_{\mathrm{amb}}}\right)), \tag{3d}$$

where the linear region is defined by $\dfrac{p_{\mathrm{im}}}{p_{\mathrm{amb}}} \in \langle \Pi_{\mathrm{lin}}, 1\rangle$ and symbols R, p_{amb}, T_{amb}, p_{im}, and γ_{air} denote constant of ideal gas, ambient pressure, ambient temperature, intake manifold pressure, and ratio of the specific heats for air, respectively. The value of Π_{lin} can be chosen according to suggestions given in Eriksson and Nielsen (2014), such that if oscillations are present in the simulated mass flow operated at the steady state and thus should be smooth, then a linear region is needed or it should be made larger. The intake manifold pressure dynamics can be described by the isotermal model given by the following equation:

$$\dot{p}_{\mathrm{im}}(\dot{m}_{\mathrm{th}}, \dot{m}_{\mathrm{ac}}) = \frac{RT_{\mathrm{im}}}{V_{\mathrm{im}}}(\dot{m}_{\mathrm{th}} - \dot{m}_{\mathrm{ac}}). \tag{4}$$

The air mass flow passing through the engine inlet valves $\dot{m}_{ac}$ is

$$\dot{m}_{\mathrm{ac}}(p_{\mathrm{im}}, N) = \eta_{\mathrm{vol}}\frac{V_{\mathrm{D}}Np_{\mathrm{im}}}{n_{\mathrm{r}}RT_{\mathrm{im}}}, \tag{5}$$

where T_{im} denotes intake manifold temperature, V_{im} is intake manifold volume, V_{D} is displacement volume for whole engine, N is engine speed, n_{r} equals to number of revolutions per one engine cycle and volumetric efficiency, η_{vol}, determines the effectiveness of the induction process of the engine. The model for volumetric efficiency (6) has been adopted from Hendricks and Sorenson (1990) and is given by:

$$\eta_{\mathrm{vol}}(p_{\mathrm{im}}, N) = \eta_{0,N} + \eta_{1,N}N + \eta_{2,N}N^2 + \eta_{1,p_{\mathrm{im}}}p_{\mathrm{im}}, \tag{6}$$

where $\eta_{0,N}$, $\eta_{1,N}$, $\eta_{2,N}$, and $\eta_{1,p_{\mathrm{im}}}$ are constant coefficients.

2.2 Fuel path dynamics

The wall wetting is a nonlinear dynamic effect that occurs in case of engines with port fuel injection. In this case, the whole amount of injected fuel m_{inj} does not enter the cylinder directly. This means that a portion of the injected fuel flow, $X\dot{m}_{\mathrm{inj}}$, is deposited as a fuel film on the wall of the intake manifold. Only the evaporated portion of the injected fuel $m_{\mathrm{fv}} = (1-X)m_{\mathrm{inj}}$ enters the cylinder directly and another portion comes from the fuel film. Hence, the fuel flow which enters the cylinder, $\dot{m}_{\mathrm{fc}}$, equals $\dot{m}_{\mathrm{fv}} + \dot{m}_{\mathrm{ff}}$ which represents the mixture of evaporated flow, $\dot{m}_{\mathrm{fv}}$, and flow from the fuel film, $\dot{m}_{\mathrm{ff}}$. The authors in Manzie et al. (2002) claim that it was experimentally verified that the wall wetting effect for a warmed engine operated under a constant temperature can be modeled with a time-varying second order system, with its parameters X and τ_{f} depending only on engine speed. Therefore, for the purposes of this paper, it is possible to utilize this relatively simple model, where the following equation:

$$\dot{m}_{\mathrm{inj}}(t_{\mathrm{inj}}, N) = NC(t_{\mathrm{inj}} - t_0), \tag{7}$$

represents model of the fuel injector with its flow capacity C and offset t_0 and the wall wetting model is given by

$$\dot{m}_{\mathrm{fv}}(t_{\mathrm{inj}}, N) = (1-X)\dot{m}_{\mathrm{inj}}, \tag{8a}$$

$$\dot{\dot{m}}_{\mathrm{ff}}(t_{\mathrm{inj}}, N, \dot{m}_{\mathrm{ff}}) = \frac{1}{\tau_{\mathrm{f}}}(X\dot{m}_{\mathrm{inj}} - \dot{m}_{\mathrm{ff}}), \tag{8b}$$

$$\dot{m}_{\mathrm{fc}}(t) = \dot{m}_{\mathrm{fv}}(t) + \dot{m}_{\mathrm{ff}}(t), \tag{8c}$$

$$X(N) = a_X N + b_X, \tag{8d}$$

$$\tau_{\mathrm{f}}(N) = a_{\tau_{\mathrm{f}}}N^{n_{\tau_{\mathrm{f}}}}. \tag{8e}$$

Typical values of parameters for this model are reported in Tab. 1. For these values, the time constant τ_{f} can vary within the range of $\langle 0.45, 0.12\rangle$ s for the engine speed of $N \in \langle 800, 6000\rangle$ rpm, and approximately 30 % of $\dot{m}_{\mathrm{inj}}$ enter cylinders directly.

2.3 Air-fuel ratio

The normalized AFR in the cylinder is defined as

$$\lambda_{\mathrm{c}}(t) = \frac{\dot{m}_{\mathrm{ac}}(t)}{\dot{m}_{\mathrm{fc}}(t)}\frac{1}{L_{\mathrm{th}}}, \tag{9}$$

where L_{th} is a value that amounts to the theoretical mass of air necessary for the ideal combustion of a unit mass of fuel. In other words this value represents the so-called stoichiometric AFR.

2.4 Gas Transport and Mixing Effect

Finally, the evolution of λ in the exhaust manifold is given by dynamics of gas mixing effect described as follows:

Table 1. Parameters of nonlinear MVEM.

Parameter	Value	Unit
τ_{th}	0.03	s
D_{th}	46×10^{-3}	m
R	280	$\mathrm{J\,kg^{-1}\,K^{-1}}$
γ_{air}	1.4	–
T_{amb}	303.15	K
p_{amb}	101.661×10^3	Pa
V_{D}	1.390×10^{-3}	$\mathrm{m^3}$
V_{im}	3.475×10^{-3}	$\mathrm{m^3}$
T_{im}	333.15	K
n_{r}	2	–
$\eta_{0,N}$	0.3	–
$\eta_{1,N}$	5×10^{-3}	–
$\eta_{2,N}$	-0.65×10^{-4}	–
$\eta_{1,p_{im}}$	0.5×10^{-5}	–
C	0.05	$\mathrm{kg\,s^{-1}}$
t_0	5×10^{-4}	s
a_X	$2\pi \times 10^{-5}$	–
b_X	0.7236	–
$n_{\tau_{\mathrm{f}}}$	-0.63	–
$a_{\tau_{\mathrm{f}}}$	$(2\pi)^{n_{\tau_f}}\,7.27$	–
L_{th}	14.64	–
τ_{mix}	0.157	s

$$\frac{\mathrm{d}}{\mathrm{d}t}\lambda_{\mathrm{em}}(t) = \frac{1}{\tau_{\mathrm{mix}}}(\lambda_{\mathrm{c}}(t-\tau_{\mathrm{d}}(N)) - \lambda_{\mathrm{em}}(t)), \tag{10}$$

where τ_{mix} denotes the time constant and

$$\tau_{\mathrm{d}}(N) = \frac{180+180+180}{360N} \tag{11}$$

is the varying transport delay occurring as the air-fuel mixture is drawn into the engine, compressed and expanded. Parameters of the particular subsystems, namely the air path, fuel path, AFR and gas mixing effect, are reported in Tab. 1 in the order as they have appeared in respective subsections.

3. OPTIMAL PWA APPROXIMATION

The authors in Kvasnica et al. (2011) address the difficulties that arise when identifying a nonlinear system in the form of PWA model directly from input-output data and propose an optimization-based approach to derive PWA approximations of nonlinear systems whose vector field is an a priori known function of multiple variables. Accordingly, the nonlinear model of the fuel path described in Subsection 2.2 can be approximated as follows. After substitution of X and τ_{f} into (8a) and (8b), the system of Eqs. (8) takes the following form:

$$\begin{aligned}\dot{m}_{\mathrm{fv}}(t_{\mathrm{inj}}, N) = {} & \overbrace{t_{\mathrm{inj}}\underbrace{(CN - b_X CN - a_X CN^2)}_{f_1}}^{1/4(f_4 - f_5)} \\ & - t_0 \underbrace{(CN - b_X CN - a_X CN^2)}_{f_1},\end{aligned} \tag{12a}$$

$$\begin{aligned}\ddot{m}_{\mathrm{ff}}(t_{\mathrm{inj}}, N, \dot{m}_{\mathrm{ff}}) = {} & \overbrace{t_{\mathrm{inj}}\underbrace{\left(\frac{a_X C}{a_{\tau_{\mathrm{f}}}} N^{(2-n_{\tau_{\mathrm{f}}})} + \frac{b_X C}{a_{\tau_{\mathrm{f}}}} N^{(1-n_{\tau_{\mathrm{f}}})}\right)}_{f_2}}^{1/4(f_6 - f_7)} \\ & - t_0 \underbrace{\left(\frac{a_X C}{a_{\tau_{\mathrm{f}}}} N^{(2-n_{\tau_{\mathrm{f}}})} + \frac{b_X C}{a_{\tau_{\mathrm{f}}}} N^{(1-n_{\tau_{\mathrm{f}}})}\right)}_{f_2} \\ & - \overbrace{\dot{m}_{\mathrm{ff}}\underbrace{\frac{1}{a_{\tau_{\mathrm{f}}}} N^{(-n_{\tau_{\mathrm{f}}})}}_{f_3}}^{1/4(f_8 - f_9)},\end{aligned} \tag{12b}$$

$$\dot{m}_{\mathrm{fc}} = \dot{m}_{\mathrm{fv}} + \dot{m}_{\mathrm{ff}}. \tag{12c}$$

Both nonlinear functions (12a) and (12b) can be converted into a separable form by applying a simple change of the variables. The first function $\dot{m}_{\mathrm{fv}}(t_{\mathrm{inj}}, N)$ is defined over a two-dimensional domain and may be rewritten into the following form:

$$\begin{aligned}\dot{m}_{\mathrm{fv}}(t_{\mathrm{inj}}, N) = {} & 1/4((t_{\mathrm{inj}} + f_1(N))^2 - (t_{\mathrm{inj}} - f_1(N))^2) \\ & + t_0 f_1(N) \\ = {} & 1/4(f_4(t_{\mathrm{inj}} + f_1(N)) - f_5(t_{\mathrm{inj}} + f_1(N))) \\ & + t_0 f_1(N),\end{aligned}$$

where t_0 is a constant, $f_4(t_{\mathrm{inj}} + f_1(N)) = (t_{\mathrm{inj}} + f_1(N))^2$ and $f_5(t_{\mathrm{inj}} - f_1(N)) = (t_{\mathrm{inj}} - f_1(N))^2$ represent quadratic functions of arguments $(t_{\mathrm{inj}} + f_1(N))$ and $(t_{\mathrm{inj}} - f_1(N))$ that are addition and subtraction of the original independent variable t_{inj} and a polynomial function $f_1(N) = (CN - b_X CN - a_X CN^2)$, respectively. Then, it is possible to approximate each nonlinear function $f_1(N)$, $f_4(t_{\mathrm{inj}} + f_1(N))$ and $f_5(t_{\mathrm{inj}} - f_1(N))$ defined over a closed domain in $\mathbb{R}$ individually, by solving the nonlinear program

$$\min_{a_i, c_i, \{r_1, \ldots, r_{S-1}\}} \quad \sum_{i=1}^{S} \left(\int_{r_{i-1}}^{r_i} (f(z) - (a_i z + c_i))^2 \, \mathrm{d}z \right) \tag{13a}$$

$$\text{s.t.} \quad r_0 \le r_1 \le \ldots \le r_{S-1} \le r_S, \tag{13b}$$

$$a_i r_i + c_i = a_{i+1} r_i + c_{i+1}, i = 1, \ldots, S-1. \tag{13c}$$

where $f(z)$ is a given nonlinear function to be approximated by S line segments. The closed domain of the function $f_1(N)$ is given by a minimum and a maximum value of the engine speed, $N_{\min}$ and $N_{\max}$, respectively. The domains of $f_4(t_{\mathrm{inj}} + f_1(N))$ and $f_5(t_{\mathrm{inj}} - f_1(N))$ are given as:

$$\begin{aligned} r_{f_4,0} &= \min\{t_{\mathrm{inj}} + f_1(N) | t_{\mathrm{inj}} \in \langle t_0, t_{\mathrm{inj,max}} \rangle \\ &\quad \wedge f_1(N) \in \langle f_1(N_{\min}), f_1(N_{\max}) \rangle\} \\ r_{f_4,S_4} &= \max\{t_{\mathrm{inj}} + f_1(N) | t_{\mathrm{inj}} \in \langle t_0, t_{\mathrm{inj,max}} \rangle \\ &\quad \wedge f_1(N) \in \langle f_1(N_{\min}), f_1(N_{\max}) \rangle\} \\ r_{f_5,0} &= \min\{t_{\mathrm{inj}} - f_1(N) | t_{\mathrm{inj}} \in \langle t_0, t_{\mathrm{inj,max}} \rangle \\ &\quad \wedge f_1(N) \in \langle f_1(N_{\min}), f_1(N_{\max}) \rangle\} \\ r_{f_5,S_5} &= \max\{t_{\mathrm{inj}} - f_1(N) | t_{\mathrm{inj}} \in \langle t_0, t_{\mathrm{inj,max}} \rangle \\ &\quad \wedge f_1(N) \in \langle f_1(N_{\min}), f_1(N_{\max}) \rangle\}. \end{aligned}$$

Since the function $f_1(N) \in \langle N_{\min}, N_{\max} \rangle$ is monotonically increasing on its domain, then it follows that $r_{f_4,0} = t_0 + f_1(N_{\min})$, $r_{f_4,S_4} = t_{\mathrm{inj,max}} + f_1(N_{\max})$, $r_{f_5,0} = t_0 - f_1(N_{\max})$ and $r_{f_5,S_5} = t_{\mathrm{inj,max}} + f_1(N_{\min})$. A similar procedure of converting to separable form and subsequent optimal approximation of $f_2(N)$, $f_6(t_{\mathrm{inj}} + f_2(N))$, $f_7(t_{\mathrm{inj}} - f_2(N))$, $f_3(N)$, $f_8(\dot{m}_{\mathrm{ff}} + f_3(N))$ and $f_9(\dot{m}_{\mathrm{ff}} - f_3(N))$ in one dimension can be applied for function (12b) as well. The graphs of all nine nonlinear functions f_i and their respective PWA approximations $\widetilde{f}_i$ are depicted in Fig. 3.

Finally, the overall optimal PWA approximations of (12a) and (12b) are given as follows:

$$\begin{aligned}\widetilde{\dot{m}}_{\mathrm{fv}}(t_{\mathrm{inj}}, N) = {} & \frac{1}{4}\left(\widetilde{f}_4\left(t_{\mathrm{inj}} + \widetilde{f}_1(N)\right) - \widetilde{f}_5\left(t_{\mathrm{inj}} - \widetilde{f}_1(N)\right)\right), \\ & - t_0 \widetilde{f}_1(N),\end{aligned} \tag{14}$$

$$\begin{aligned}\widetilde{\ddot{m}}_{\mathrm{ff}}(t_{\mathrm{inj}}, N, \dot{m}_{\mathrm{ff}}) = {} & \frac{1}{4}\left(\widetilde{f}_6\left(t_{\mathrm{inj}} + \widetilde{f}_2(N)\right) - \widetilde{f}_7\left(t_{\mathrm{inj}} - \widetilde{f}_2(N)\right)\right) \\ & - \frac{1}{4}\left(\widetilde{f}_8\left(\dot{m}_{\mathrm{ff}} + \widetilde{f}_3(N)\right) - \widetilde{f}_9\left(\dot{m}_{\mathrm{ff}} - \widetilde{f}_3(N)\right)\right) \\ & - t_0 \widetilde{f}_2(N).\end{aligned} \tag{15}$$

To validate obtained approximations, open-loop simulations were performed and results are shown in Fig. 4. The open-loop response of a very precise approximation $\widetilde{\dot{m}}_{\mathrm{fc}}$ of $\dot{m}_{\mathrm{fc}}$, with the following numbers of segments of each approximated function $S_1 = 3$, $S_2 = 25$, $S_3 = 25$, $S_4 = 25$, $S_5 = 25$, $S_6 = 25$, $S_7 = 25$, $S_8 = 15$ and $S_9 = 25$ is represented by the solid blue line. Let us denote the total number of line segments as $\overline{S} = \sum_i S_i$ and the associated model by $\widetilde{m}, \overline{S} = 193$ for the referring purposes in the further text. As can be seen from this result, open-loop response of this approximation perfectly matches the open-loop response of nonlinear model represented by the solid red line. Naturally, approximations of lower complexity provide open-loop response of lower accuracy, e.g. open-loop response of approximation with following segmentation: $S_1 = 1$, $S_2 = 3$,

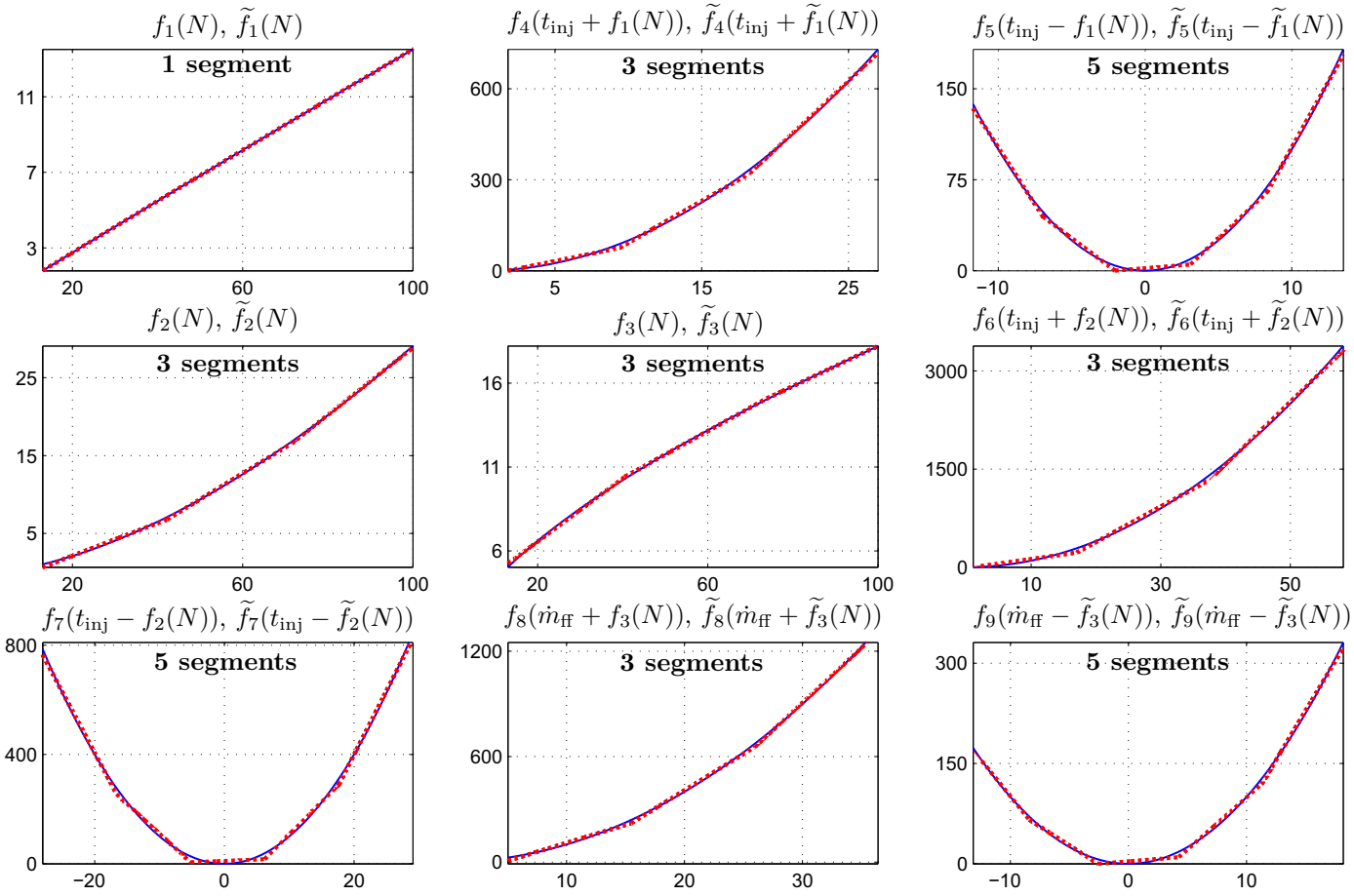

Fig. 3. Nonlinear functions (blue) and their PWA approximations (red)

$S_3=3$, $S_4=3$, $S_5=5$, $S_6=3$, $S_7=5$, $S_8=3$ and $S_9=5$, is depicted by the dashed blue line in Fig. 4. Similarly, let us denote this model as $\widetilde{m}, \overline{S}=31$. Nevertheless, due to the closed-loop nature of MPC strategy using even approximations with lower accuracy can provide satisfactory control performance, as will be shown in Section 5.

4. CONTROLLER FORMULATION

The best achievable performance of air-fuel ratio control in terms of the highest efficiency of the three way catalytic conversion is when $\lambda_{\rm c}$ is kept on the stoichiometric level. Therefore, it is sensible to track the reference trajectory given by $\dot{m}_{\rm ac}(t)/L_{\rm th}$ and for AFR MPC controller synthesis, as proposed in this paper, the model of air path dynamics is used in order to predict the evolution of air mass flow into the cylinder $\dot{m}_{\rm ac}(t)$, where referenced throttle position $\alpha_{\rm ref}$ together with engine speed N are treated as measured disturbances. The model of the fuel path dynamics is incorporated into the MPC scheme in order to predict optimal trajectories of fuel injection time $\mathbf{t}^{\star}_{\rm inj}(\cdot)$ as manipulated variable and fuel mass flow $\dot{\mathbf{m}}^{\star}_{\rm fc}(\cdot)$ as controlled variable. The given optimal control problem (16) is solved at each sampling instant $t=kT$, where only the first element of the optimizer, $t^{\star}_{\rm inj}(0)$, is applied to the controlled plant. The constraints in (16b)-(16g) are imposed $\forall k=0,\dots,N_{\rm c}-1$ with $N_{\rm c}$ denoting prediction horizon. The objective is to minimize the weighted square of tracking error , accompanied with integral action, to reject the unmodeled effects. The tradeoff between obtaining an aggressive tracking performance and a smooth profile of the manipulated variable can be achieved by appropriately adjusting tuning parameters Q, Q_i, and R.

$$\min_{\mathbf{t}_{\rm inj}(\cdot)} \quad \sum_{k=0}^{N_{\rm c}-1} Q\left(\frac{\dot{m}_{{\rm ac}_{t|t+kT}}}{L_{\rm th}}-\dot{m}_{{\rm fc}_{t|t+kT}}\right)^2+Q_{\rm i}d^2_{t|t+kT} + R\left(t_{{\rm inj}_{t|t+kT}}-t_{{\rm inj}_{t|t+(k-1)T}}\right)^2 \tag{16a}$$

$$\text{s.t.} \quad N_{t|t+kT}=N_{t|t+(k-1)T}+(N_t-N_{t-T}), \tag{16b}$$

$$\dot{m}_{{\rm ff}_{t|t+kT}}=\dot{m}_{{\rm ff}_{t|t+(k-1)T}}+T\widetilde{\dot{m}}_{{\rm ff}_{t|t+(k-1)T}}, \tag{16c}$$

$$\dot{m}_{{\rm fc}_{t|t+kT}}=\widetilde{\dot{m}}_{{\rm fv}_{t|t+kT}}+\dot{m}_{{\rm ff}_{t|t+kT}}, \tag{16d}$$

$$d_{t|t+kT}=d_{t|t+(k-1)T}+\left(\frac{\dot{m}_{{\rm ac}_{t|t+kT}}}{L_{\rm th}}-\dot{m}_{{\rm fc}_{t|t+kT}}\right), \tag{16e}$$

$$t_0\le t_{{\rm inj}_{t|t+kT}}\le 5\,{\rm ms} \tag{16f}$$

$$e_{\rm lb}\le\left(\dot{m}_{{\rm ac}_{t|t+kT}}/L_{\rm th}-\dot{m}_{{\rm fc}_{t|t+kT}}\right)\le e_{\rm ub},. \tag{16g}$$

The optimal control problem (16) was formulated using YALMIP (Löfberg, 2004) and subsequently solved online as a mixed-integer quadratic problem (MIQP) with the GUROBI solver (Gurobi Optimization, Inc., 2015). The terms $\widetilde{\dot{m}}_{{\rm fv}_{t|t+kT}}$ and $\widetilde{\dot{m}}_{{\rm ff}_{t|t+(k-1)T}}$ in constraints (16d) and (16c) denote predictions using the PWA approximations given by (14) and (15), with dependencies on arguments, i.e. $\widetilde{\dot{m}}_{{\rm fv}_{t|t+kT}}=\widetilde{\dot{m}}_{\rm fv}(t_{{\rm inj}_{t|t+kT}},N_{t|t+kT})$ and $\widetilde{\dot{m}}_{{\rm ff}_{t|t+(k-1)T}}=\widetilde{\dot{m}}_{\rm ff}(t_{{\rm inj}_{t|t+(k-1)T}},N_{t|t+(k-1)T},\dot{m}_{{\rm ff}_{t|t+(k-1)T}})$. The symbol $d_{t|t+kT}$ in (16a) and (16e) stands for pre-

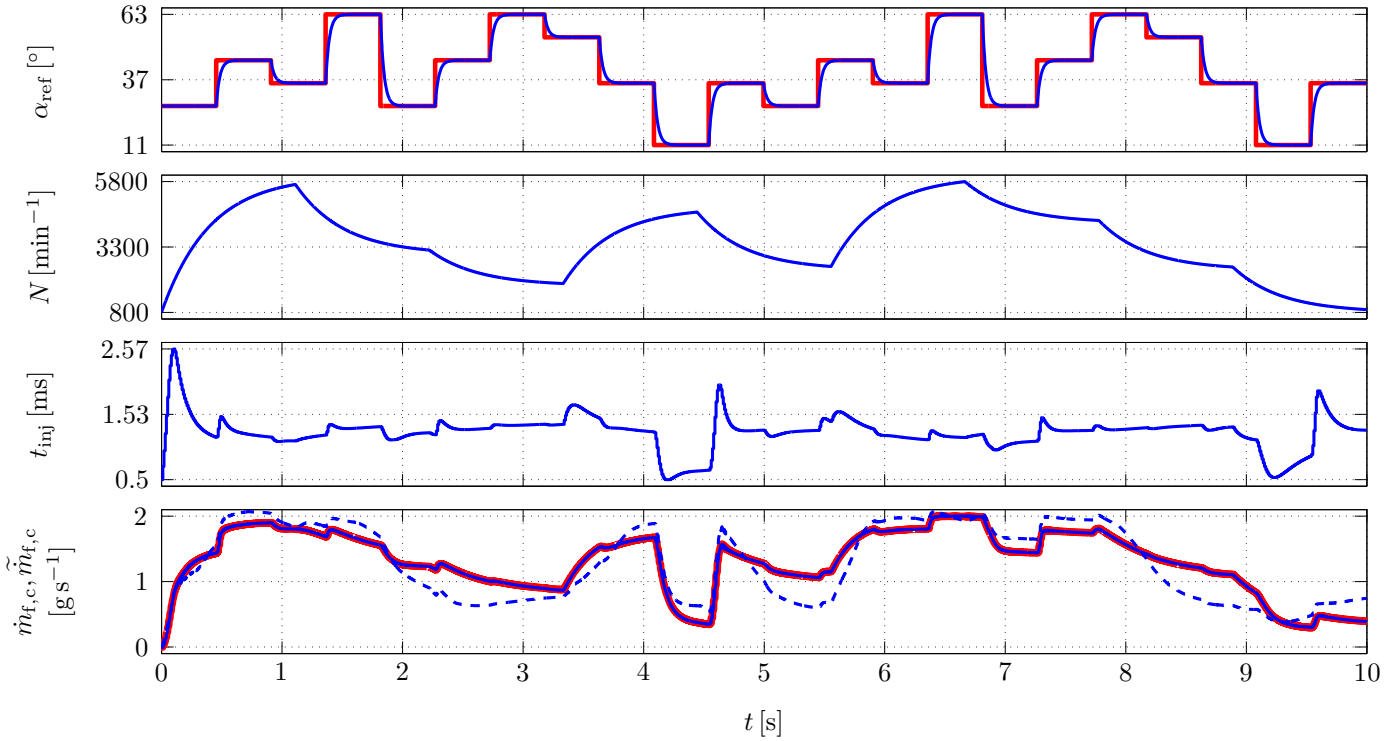

Fig. 4. PWA model validation, response of nonlinear model (red) and PWA approximations (solid/dashed blue)

dictions of integral variable. The constraint (16b) determines the evolution of engine speed over the prediction horizon with a constant rate. Finally, the inequalities in (16f) and (16g) correspond to constraints imposed on the manipulated and the controlled (using appropriate bounds e_{lb}, e_{ub}) variable, respectively, **so as to achieve their smoother profiles. . . .**

As a reference, the same optimization problem was solved to obtain an NMPC controller, yet by exploiting the fully nonlinear fuel path dynamics model in (16c) and (16d). To achieve this, the underlying control problem was solved as an NLP using the technique of sequential quadratic programming (SQP) implemented in MATLAB's `fmincon` featuring warm-start initialization.

5. SIMULATION RESULTS

In order to keep the computation effort low, let us quantify the control performance for both NMPC and the hybrid MPC assuming the prediction horizon of $N_{\mathrm{c}} = 2$ steps and the sample time of $T = 10\,\mathrm{ms}$. Note that this value is sufficient since the controlled variable $\dot{m}_{\mathrm{fc}}$ is directly dependent on the manipulated variable t_{inj}, due to the fact that approximately one third of the injected fuel mass flow $\dot{m}_{\mathrm{inj}}$ enters the cylinder directly. The performance can be assessed in terms of achievable tracking performance by evaluating an integral criterion in the form of $J_{\dot{m}} = \int_0^t (\dot{m}_{\mathrm{ac}}(\tau)/L_{\mathrm{th}} - \dot{m}_{\mathrm{fc}}(\tau))^2 \mathrm{d}\tau$ or the ability to keep λ close to 1 by evaluating the criterion $\mathrm{J}_\lambda = \int_0^t (\lambda_{\mathrm{em}}(\tau) - 1)^2 \mathrm{d}\tau$. Accordingly, the performance of three equivalently tuned controllers, $N_{\mathrm{c}} = 2$, $Q = 10$, $Q_{\mathrm{i}} = 10$, $R = 1$, are shown in Fig. 5, where both disturbance signals, throttle position $\alpha(t)$ and engine speed $N(t)$ vary in predefined intervals to excite the engine within its entire operating range. All the three controllers exhibit a very good performance, i.e. only small deviations of λ_{em} from 1, less than ± 0.3 are present and persist only for a short time, except for larger deviations at the beginning of the simulation caused by starting the computations from specific initial conditions.

The best performance is clearly achieved when employing the proposed hybrid MPC using optimal PWA approximation of a relatively high complexity, represented by the solid blue lines depicting the manipulated variable t_{inj} and controlled variable λ_{em}, which comes at a price of higher values of the task execution time (TET). Let us denote this hybrid MPC as $\mathrm{hMPC}_{\widetilde{m},\overline{S}=193}$, referring to utilizing the model previously denoted as $\widetilde{m}, \overline{S} = 193$. The performance of a similarly denoted hybrid MPC controller $\mathrm{hMPC}_{\widetilde{m},\overline{S}=31}$ and NMPC are represented by dashed blue lines and solid red lines, respectively.

The above performance indicators are reported in Tab. 2. As it can be seen from the results, the hybrid MPC controller $\mathrm{hMPC}_{\widetilde{m},\overline{S}=31}$, using optimal PWA approximation with a rather modest segmentation, exhibits comparable tracking performance as NMPC while achieving a lower average task execution time $\mathrm{TET}_{\mathrm{avg}}$. Overall, the computation times of the investigated hMPC variants scale as expected, while offering a reasonable tradeoff between performance accuracy and runtime effort, with respect to a desired complexity of the employed optimal PWA approximation. We remark that the simulations were performed on a machine equipped with Intel i5-3317U CPU and 8GB of RAM.

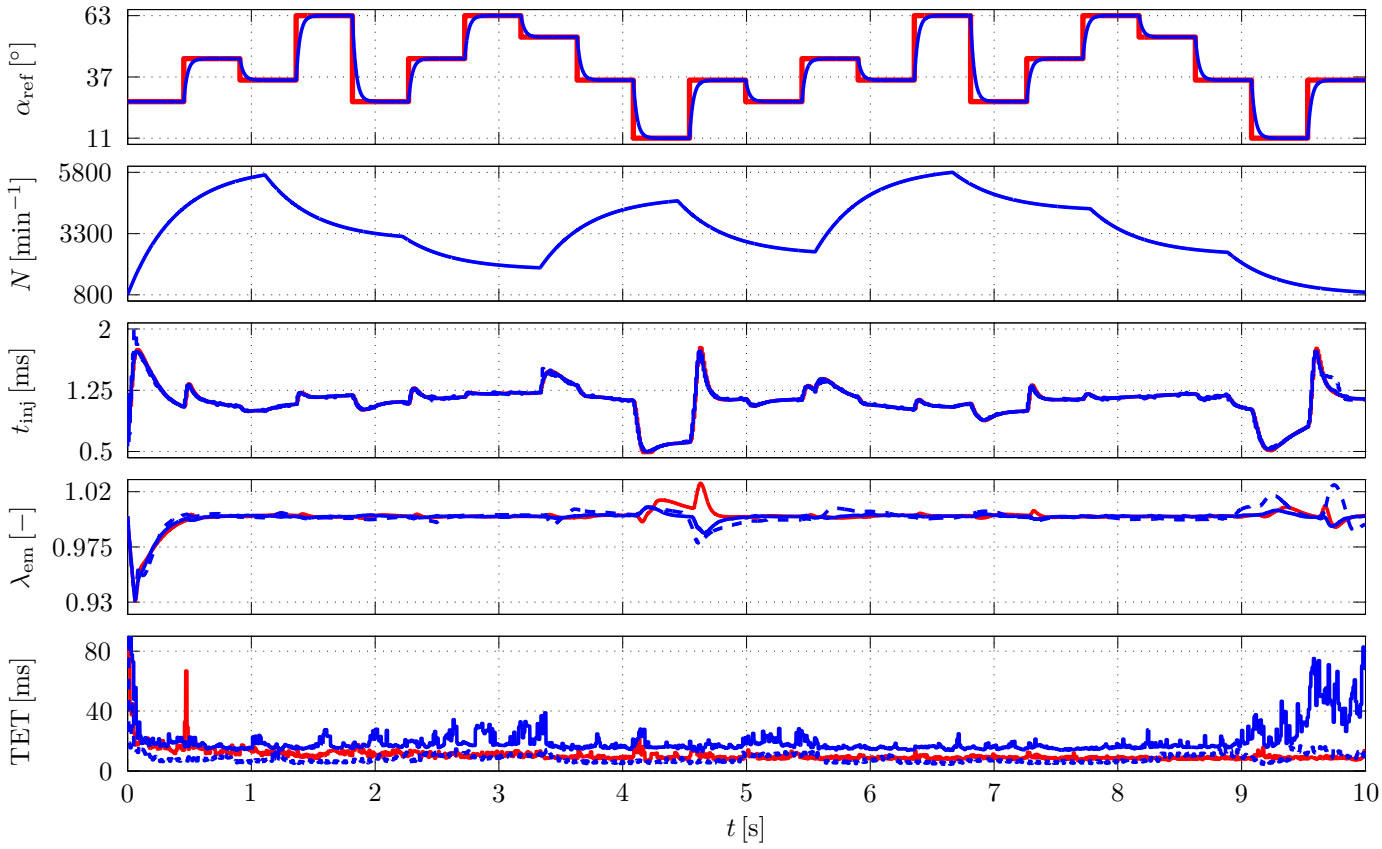

Fig. 5. Simulation results for three equally tuned controllers, $N_{\text{c}} = 2$, $Q = 10$, $Q_{\text{i}} = 10$, $R = 1$. The solid red lines represents NMPC performance, solid blue lines hMPC$_{\tilde{\dot{m}},\overline{S}=193}$ and dashed blue lines hMPC$_{\tilde{\dot{m}},\overline{S}=31}$

Table 2. Control performance assessment

	$J_{\dot{m}} \times 10^{-9}$ [–]	$J_{\lambda} \times 10^{-4}$ [–]	TET_{avg} [ms]
hMPC$_{\tilde{\dot{m}},\overline{S}=193}$	1.0154	4.6648	19.2
hMPC$_{\tilde{\dot{m}},\overline{S}=163}$	1.0220	4.6666	16.1
hMPC$_{\tilde{\dot{m}},\overline{S}=132}$	1.0225	4.6735	14.1
hMPC$_{\tilde{\dot{m}},\overline{S}=80}$	1.0393	4.7647	10.8
hMPC$_{\tilde{\dot{m}},\overline{S}=51}$	1.4915	5.1514	9.4
hMPC$_{\tilde{\dot{m}},\overline{S}=31}$	2.9070	6.9379	8.4
NMPC	2.2535	5.2828	9.8

6. CONCLUSION

This paper presented an optimal PWA approximation of the nonlinear fuel path model of a gasoline combustion engine, enabling to design an online hybrid MPC for the air-fuel ratio control. Specifically, the underlying MPC problem was formulated to track the fuel mass flow reference in cylinder so as to keep the AFR as close as possible to the stoichiometric value. The controller performance was evaluated using several optimal PWA approximations of a different complexity. It was shown that the resulting MIQP-based hybrid MPC controller using a more precise approximation allows for a better control performance than an NLP-based NMPC controller, yet at a price of a higher computation time. Nevertheless, it was shown that a comparable runtime complexity and AFR control performance can be achieved even for a very coarse PWA approximation. This makes the proposed approach a possible alternative to NMPC strategies, with potential to be exploited in embedded control applications, explicit MPC framework etc.

REFERENCES

del Re, L., Allgöwer, F., Glielmo, L., Guardiola, C., and Kolmanovsky, I. (2009). *Automotive Model Predictive Control: Models, Methods and Applications.* Springer Verlag.

Eriksson, L. and Nielsen, L. (2014). *Modeling and Control of Engines and Drivelines.* John Wiley & Sons, Ltd.

Gurobi Optimization, Inc. (2015). Gurobi optimizer reference manual. Available at: `http://www.gurobi.com`.

Guzzella, L. and Onder, C. (2010). *Introduction to modeling and control of internal combustion engine systems.* Springer-Verlag Berlin Heidelberg.

Hendricks, E. and Sorenson, S. (1990). Mean value si engine model for control studies. In *Amer. Control Conf.*, 1882–1887.

Honek, M., Kvasnica, M., Szücs, A., Šimončič, P., Fikar, M., and Rohaľ-Ilkiv, B. (2015). A low-complexity explicit MPC controller for AFR control. *Control Eng. Pract.*, 42, 118–127.

Kvasnica, M., Szücs, A., and Fikar, M. (2011). Automatic derivation of optimal piecewise affine approximations of nonlinear systems. *IFAC Proc. Volumes*, 44(1), 8675–8680. 18th IFAC World Congress.

Löfberg, J. (2004). YALMIP: a toolbox for modeling and optimization in MATLAB. In *IEEE Int. Symp. Comput. Aided Control Syst. Design*, 284–289.

Manzie, C., Palaniswami, M., Ralph, D., Watson, H., and Yi, X. (2002). Model predictive control of a fuel injection system with a radial basis function network observer. *J. Dyn. Syst. Meas. Contr.*, 124(4), 648–658.

Rupp, D. and Guzzella, L. (2010). Adaptive internal model control with application to fueling control. *Control Eng. Pract.*, 18(8), 873–881.

Shen, T., Zhang, J., Jiao, X., Kang, M., Kako, J., and Ohata, A. (2015). *Transient Control of Gasoline Engines*. CRC Press.

Wang, S., Yu, D., Gomm, J., Page, G., and Douglas, S. (2006). Adaptive neural network model based predictive control for air-fuel ratio of SI engines. *Eng. Appl. Artif. Intell.*, 19(2), 189–200.

Wojnar, S., Polóni, T., Šimončič, P., Rohaľ-Ilkiv, B., Honek, M., and Csambál, J. (2013). Real-time implementation of multiple model based predictive control strategy to air/fuel ratio of a gasoline engine. *Arch. Control Sci.*, 23(1), 93–106.

Zhai, Y.J., Yu, D.L., Tafreshi, R., and Al-Hamidi, Y. (2011). Fast predictive control for air-fuel ratio of SI engines using a nonlinear internal model. *Int. J. Eng. Sci. Technol.*, 3(6), 1–17.

Zhai, Y.J., Yu, D.L., and Wang, K.L. (2007). Comparison of single-dimensional and multi-dimensional optimization approaches in adaptive model predictive control for air-fuel ratio of SI engines. *Int. J. Inf. Syst. Sci.*, 3(1), 129–149.

Zope, R., Mohammadpour, J., Grigoriadis, K., and Franchek, M. (2010). Robust fueling strategy for an SI engine modeled as an linear parameter varying time-delayed system. In *Proc. 2010 Am. Control Conf.*, 4634–4639.